Magnetic breakdown in periodically Si-doped GaAs

A. B. Henriques and V. N. Morgoon*
Instituto de Física da Universidade de São Paulo, Caixa Postal-20516, 01498-970 São Paulo, Brazil

P. L. de Souza
Centro de Estudos em Telecomunicações, Pontifícia Universidade Católica, 22453 Rio de Janeiro, Brazil

V. Bindilatti, N. F. Oliveira, Jr., and S. M. Shibli
Instituto de Física da Universidade de São Paulo, Caixa Postal-20516, 01498-970 São Paulo, Brazil
(Received 3 November 1993)

The conduction band electronic structure in periodically Si-doped GaAs was studied by Shubnikov–de Haas measurements in tilted fields of 0–14 T. The samples had a doping period of 140 Å and 220 Å, with a sheet carrier density per superlattice period of 2.8×10^{12} cm^{-2} and 2.2×10^{12} cm^{-2}, respectively. The periodicity and the intensity of the oscillations in the magnetoresistance, as a function of the tilt angle, follow accurately the theoretical values obtained from a self-consistent calculation of the Fermi surface. An extra period appears in the spectra when the magnetic-field direction is tilted away from the axis of the superlattice, which is seen as a peak in the Fourier transform of the oscillations. The angular dependence of the position and of the intensity of this peak allows us to establish that it arises because of magnetic breakdown.

INTRODUCTION

The development of semiconductor epilayer growth techniques has allowed researchers to obtain semiconductor materials with a degenerate electron gas in which the quantum-mechanical potential is tailored to achieve a spatial modulation of the density distribution of free carriers. In periodically Si-spike-doped GaAs, sheets of substitutional Si atoms, described by an areal density N_d, are introduced into equally spaced planes of the GaAs crystal. The electrons released from the shallow Si donors are confined by a periodic space-charge potential, of periodicity equal to the spacing between the dopant sheets, a. The conduction band electrons occupy a volume of phase-space equal to $\frac{4}{3}\pi k_F^3$, where $k_F = 3\pi^2 n_S/a$, and $n_s \approx N_d$ if $N_d < 2.0 \times 10^{13}\text{cm}^{-2}$.[1] This volume of phase space is centered around the Γ point of the GaAs Brillouin zone, hence the effective mass theory will be appropriate to describe the conduction band electrons, which can be seen as an effective mass electron gas confined by a periodic potential in one dimension. As pointed out by Koch and co-workers, periodically Si-doped GaAs can be described by its Fermi surface.[2] For the short-period superlattice, the electric quantum limit can be achieved, in which case the Fermi surface approaches a sphere. When the spacing between the dopant sheets is increased, the number of populated minibands increases, in which case the Fermi surface will contain separate unconnected sections. The gradual change in the shape of the Fermi surface which occurs when the spacing between the donor sheets is reduced reflects the crossover from a dimensionality of 2 to 3.[3]

Recently, experimental studies of periodically Si-doped GaAs[1,4] and $InAs_{1-x}Sb_x$/InSb strained-layer superlattices[5] by the Shubnikov–de Haas effect (SdH) were performed, and the occurrence of magnetic breakdown (MB) was suggested. In our previous investigation,[4] magnetoresistance (MR) oscillations were seen, which were tentatively attributed to the MB effect, although no extensive study was made. In the present work the MB effect is investigated in the light of self-consistent calculations of the Fermi surface for each sample. The accuracy of the theoretical calculations is demonstrated by the good agreement between the theoretical and experimental extremal cross sections of the Fermi surface. The theoretical model also allows us to estimate the frequencies of the MR oscillations associated with the magnetic breakdown effect, and good quantitative agreement is obtained with the experimentally observed MB oscillatory magnetoresistance.

The MR oscillations were studied as a function of the tilt angle (the angle between the magnetic-field direction and the axis of symmetry of the superlattice). The Fourier transform of the experimental MR oscillations, plotted in inverse magnetic field, displays peaks centered at the fundamental magnetic-field values B_F, which are related to the extremal cross sections of the Fermi surface in a plane perpendicular to the field direction A_e, through the relation $B_F = \hbar A_e/2\pi e$. The Fourier peak positions obtained from the experiment are directly compared to the calculated extremal cross sections of the Fermi surface. The theoretical calculations included the exchange-correlation correction in the local density approximation, and the conduction band nonparabolicity; details of the theoretical procedures are given in Ref. 3.

EXPERIMENT

The samples were grown on (100) GaAs undoped semi-insulating substrates in a Varian GEN II molecular-beam

epitaxy (MBE) system. An undoped GaAs buffer layer was grown before doping. The intended doping level was approximately $N_d \simeq 2.5 \times 10^{12}$ cm^{-2}. The spacing between the dopant layers was measured by a C–V P4300 profiler, with an estimated error of ±10 Å. The Shubnikov–de Haas measurements were made using a four-contact geometry; the samples were approximately square, with four contacts in the corners. The MR oscillations were studied at a fixed temperature of $T = 4.2$ K in magnetic fields up to 14 T. The sample holder allowed for rotation of the sample, and the direction of the magnetic field relative to the superlattice axis was established with an accuracy better than 1°. Hall measurements at 4.2 K were performed using the van der Pauw technique, and the average Hall mobility was approximately 3500 cm^2/Vs for all samples.

RESULTS AND DISCUSSION

Figures 1(a) and 2(a) depict the MR traces of the samples studied (no. 1, with a superlattice period of $a = 140$ Å, and no. 2, with $a = 220$ Å), for a magnetic field parallel to the growth direction (tilt angle θ=0). Figures 1(b) and 2(b) show the Fourier spectrum of the second derivative (plotted in $1/B$) of the oscillations shown in Figs. 1(a) and 2(a), respectively. (The frequency, which is the inverse of the period of the oscillations, is given in units of T). For both samples, two periods are detected. The Fermi surface can be represented by its rotationally symmetric cross section, shown in Fig. 3 for both samples. In the theoretical calculation of the Fermi surface, the input parameters were the superlattice period a and the sheet carrier density n_S. The carrier density n_S was the single adjustable parameter, used to obtain the best match between the measured Fourier frequencies and the calculated extremal cross sections of the Fermi surface. The Fermi surface contains two separate sections: a cylindrical one, with a modulated cross section, due to the occupation of the fundamental miniband, and a lens-shaped one, due to the occupation of the second miniband. For sample no. 2, a small pocket due to electrons in a third miniband is predicted theoretically; however, the energy gap between the second and third minibands is only 0.7 meV, which is much less than the level broadening (see

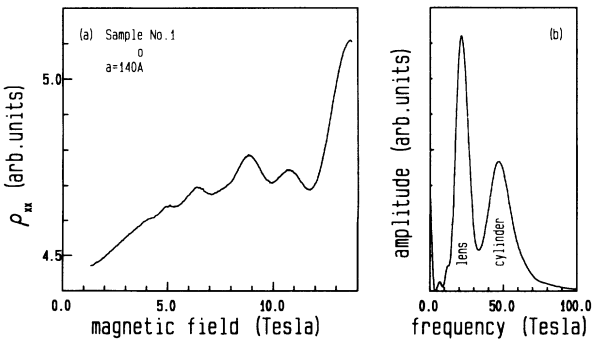

FIG. 1. Experimental trace of the SdH oscillations (a) and Fourier transform (b) for sample no. 1.

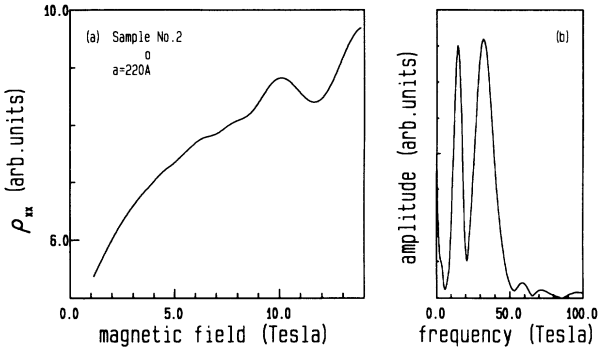

FIG. 2. Experimental trace of the SdH oscillations (a) and Fourier transform (b) for sample no. 2.

below), and can be ignored. At $\theta = 0°$, three extremal circular cross sections exist: a "belly" at k_z=0 and a "neck" frequency at $k_z = \pi/a$, due to the modulated cylinder, and the cross section of the lenslike surface at $k_z = \pi/a$, thus implying that three peaks should be detected in the Fourier spectrum. It can be demonstrated, however, that when the level broadening γ is larger than or approximately equal to the width Γ of the miniband, the belly and the neck cross sections will not be resolved separately, but as a single oscillatory component, which can be approximated by the average value of the belly and neck cross sections.[7] The level broadening at the Fermi energy is related to the Dingle temperature T_D, which was estimated from the experimental MR traces, through $\gamma = \pi k_B T_D$. By bandpass filtering the Fourier transform of the MR traces, each group of oscillations was separated from the background spectrum, and for each group T_D was extracted from the field dependence of the amplitude of the oscillations; the numerical procedure is equivalent to the one described in Ref. 8. This showed that the level broadening was approximately equal to, or larger than the calculated width of the first miniband, thus making the belly and neck frequencies unresolved. Table I summarizes the results of the calculations and the measured level broadening for both samples.

The angular dependence of the Fourier spectrum for

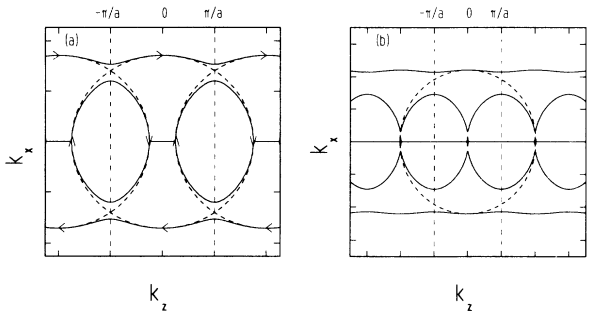

FIG. 3. Cross section of the Fermi surface for sample no. 1 (a) and sample no. 2 (b). Dashed lines show the breakdown orbit at $\theta = 90°$. Vertical lines are the limits of the mini-Brillouin-zone. Both figures enclose the same area of phase space (0.05^2 Å^{-2}).

TABLE I. Carrier density per superlattice period, as obtained from the analysis of the zero-tilt-angle SdH spectra. The calculated width of the lowest-energy miniband (Γ) and energy gap to the next miniband (Δ). The Fermi energy E_F is given relative to the bottom of the fundamental miniband. γ_1 and γ_2 are the values of the broadening of the Landau levels for the first and second minibands, estimated from the SdH spectra for $\theta = 0°$. B_0 is the magnetic-field intensity which determines the tunneling probability (see text).

Sample	SL period a (Å)	n_S (cm^{-2})	Γ (meV)	Δ (meV)	E_F (meV)	$\gamma_1 = \pi k_B T_D$ (meV)	γ_2 (meV)	$B_0 = \frac{m^* \Delta^2}{\hbar e E_F}$ (T)
No. 1	140	2.8×10^{12}	15.4	24.1	78.1	13.9	5.7	4.8
No. 2	220	2.2×10^{12}	3.0	27.3	54.0	15.0	5.2	9.2

the sample no. 1 is shown in Fig. 4. The peak positions detected in the spectra of Fig. 4 are shown by circles in Fig. 5; the area of each circle is a measure of the relative intensity of the corresponding peak. It is seen that the high-frequency peak (due to the orbit in the cylindrical surface) is displaced to higher fields as the tilt angle increases, as expected for an open Fermi surface, whereas the low-frequency peak (due to the extremal orbit in the lens-shaped surface), is displaced to lower fields, also as expected. The theoretical angular dependence of the position of these peaks, shown by solid lines in Fig. 5, is in excellent agreement with the experimental values. The dependence of the amplitude of the oscillations on the tilt angle observed can also be described quantitatively by the theory. As the tilt angle increases, the cyclotron mass $m_c(\theta) = \frac{\hbar^2}{2\pi} \frac{dA_e(\theta)}{dE_F}$ increases for the extremal orbit in the cylindrical surface, which reduces the cyclotron frequency, and when $\omega_c \tau > 1$, where $\tau = \hbar/\gamma_1$, is no longer attained within the range of fields in our experiment ($B \leq 14$ T), the corresponding oscillations are no longer detected experimentally. The cyclotron mass was calculated theoretically, and we estimated the high-frequency peak to vanish from our spectra when $\theta > 50°$, in good agreement with the experiment. In contrast, the cyclotron mass decreases for the orbit in the lens-shaped surface, and the amplitude of the oscillations due to this orbit increases, in agreement with the theory.

However, for sample no. 1, for a tilt angle θ larger than 40°, a peak of frequency close to the high-frequency peak, observed for $\theta = 0°$, reappears in the spectrum, and at $\theta = 90°$ attains an intensity comparable to the one detected at $\theta = 0°$. The reappearance of the high-frequency peak was also seen for sample no. 2, although it is much weaker than for sample no. 1, and the frequency was notably lower than that of the $\theta = 0°$ high-frequency peak. The reappearance of the high-frequency peak when the sample is rotated cannot be explained within the framework of the semiclassical theory, which predicts only the lens-shaped orbit for $\theta = 90°$, and is attributed to the MB effect.[6] For electrons confined by a one-dimensional periodic potential, the theory of the MB effect was described by Pippard[9] and Stark and Falicov.[10] The "closing network" of coupled orbits consists of a pair of open orbits [shown by arrows in the modulated cylinder section of the Fermi surface in Fig. 3(a)], which are closed via smaller linking orbits [shown by arrows in the lens-shaped section of the Fermi surface in Fig. 3(a)], to give at MB a large closed orbit [shown by dashed lines in Fig. 3(a)], whose diameter exceeds the size $2\pi/a$ of the mini-Brillouin-zone. If phase coherence of the electron wave function is maintained along the MB orbit, the closing network will give rise to MR oscillations whose frequency is related to the area enclosed by the orbit as before, i.e., $B_F = \hbar A_e / 2\pi e$. The field and temperature dependence of the amplitude of the MB oscillations in the transverse MR for the closing network was given by Young:[11]

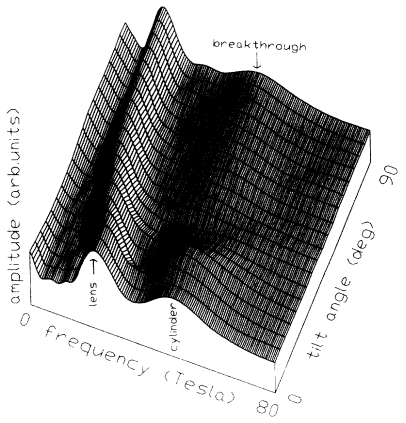

FIG. 4. Angular dependence of the Fourier transform of the SdH oscillations for sample no. 1. Peaks corresponding to the semiclassical orbits in the cylindrical and lens-shaped sections of the Fermi surface, and the breakdown orbit, are indicated.

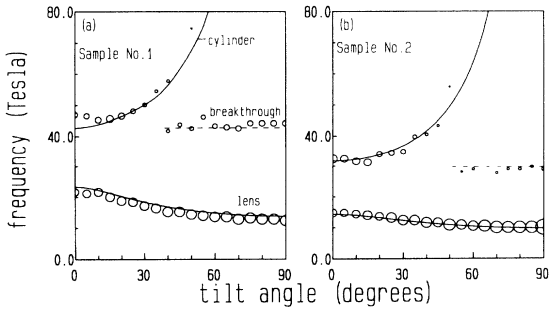

FIG. 5. Peak positions (circles) detected in the Fourier transform for sample no. 1 (a) and sample no. 2 (b). The solid lines are the extremal cross sections of the cylindrical and lenslike sections of the Fermi surface. The dashed line is the calculated area of the breakdown orbit.

$$A \sim \frac{T}{B} \exp\left\{-\frac{2\pi^2 k_B (T + T_D')}{\hbar\omega_c} - \frac{B_0}{B}\right\} \qquad (B \lesssim B_0), \tag{1}$$

where $B_0 = \frac{m^* \Delta^2}{\hbar e E_F}$ is the intensity of the magnetic field at which the probability of tunneling between the cylinder-shaped surface and the lens-shaped one, $P = \exp(-B_0/B)$, becomes relevant. We find the MB oscillations to be well approximated by Eq. (1); however, we could not estimate B_0 from a fit of (1) to the experimental oscillations because of the unknown value of T_D'. T_D' is a measure of the scattering rate of electrons orbiting in a plane perpendicular to the Si sheets, which is different from T_D (Table I), which measures the rate of scattering in an orthogonal plane. However, using the theoretical parameters given in Table I, we can obtain theoretical estimates of $B_0 = 8.3$ T for sample no. 2, but only 4.5 T for sample no. 1. Thus, the much stronger reappearance of the circular orbits in the 140-Å sample at $\theta \approx 90°$ than in the 220-Å sample is consistent with the hypothesis of MB. Moreover, it can be seen that the Fourier frequency corresponding to the breakdown orbit is nearly the same as the semiclassical one for the sample no. 1, whereas for sample no. 2 the breakdown Fourier frequency is less than the semiclassical one. This is exactly what we would expect, since for sample no. 2 the electrons are more tightly bound to a given well,[3] leading to a larger deviation from the nearly-free-electron model than for sample no. 1. As Fig. 3 shows, while for sample no. 1 the breakdown orbit is nearly circular, for sample no. 2 the orbit is elliptical, covering a smaller area than the semiclassical orbit, predicted for $\theta = 90°$.

When the tilt angle is decreased from 90°, the tunneling of electrons through the gap in k space between the open and closed semiclassical trajectories, Δk, will persist as long as these trajectories can be linked by a free-electron trajectory. Figure 6 shows the calculated semiclassical trajectories as a function of the tilt angle for sample no. 1. We find that such a linkage can be traced if $90° \geq \theta \gtrsim 40°$; in this interval of values of θ, the gap Δk changes weakly. These theoretical results indicate that the MB effect should only be observed if the tilt angle is greater than $\simeq 40°$, and above this value of θ the amplitude of the MB oscillations should be little sensitive to the tilt angle, in good agreement with the experimental observations.

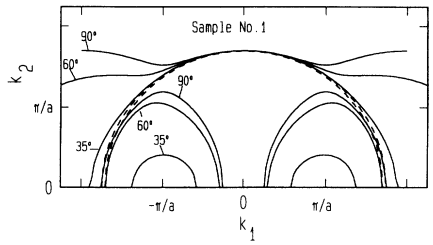

FIG. 6. Semiclassical electron trajectories (solid lines) for sample no. 1, as a function of the tilt angle. Dashed lines are the breakdown orbits for 90° and 60°. k_1 and k_2 are the wave vector components perpendicular to the field direction.

CONCLUSION

In summary, the good overall agreement between theory and experiment, shown in this work, demonstrates that the Fermi surface of short-period periodically Si-doped GaAs can be modeled theoretically with a high degree of accuracy. We have presented conclusive evidence of the occurrence of the effect of magnetic breakdown in periodically Si-doped GaAs, which corresponds very much to the idealized simplest systems of nearly free electrons in a periodic potential in one dimension. The observation of oscillations for the closing network indicates that coherent magnetic breakdown takes place in our samples.[12,13] It is worthy of notice that magnetic breakdown occurs when the electronic structure is intermediate between two and three dimensional, and the Fermi surface is neither cylindrical (2D) nor spherical (3D). The observation of magnetic breakdown in semiconductor superlattices, which can be shaped within a wide range by adjusting the design parameters, makes them promising for the observation of such effects as nonlinear conductivity and quantum localization of electrons under magnetic breakdown conditions, which are predicted theoretically.[12]

ACKNOWLEDGMENTS

This work was sponsored by the government agencies FAPESP and CNPq. One of us (V.N.M.) was supported by FAPESP Grant. No. 92/3681–0.

*Permanent address: Kharkov State University, Department of Physics, 4 Svobody Square, 310077 Kharkov, Ukraine.

[1] R. Droopad, S.D. Parker, E. Skuras, R.A. Stradling, R.L. Williams, R.B. Beall, and J.J. Harris, in *Magnetic Fields in Semiconductor Physics II, Transport and Optics,* Proceedings of the International Conference, Würzburg, Germay, 1988, edited by G. Landwehr, Springer Series in Solid-State Sciences Vol. 87 (Springer-Verlag, Berlin, 1989), p. 199.

[2] F. Koch, A. Zrenner, and M. Zachau, in *Two Dimensional Systems: Physics and New Devices,* Proceedings of the International Winter School, Mauterndorf, Austria, 1986, edited by G. Bauer, F. Kuchar, and H. Heinrich, Springer Series in Solid-State Sciences Vol. 67 (Springer-Verlag, Berlin, 1986), p. 175.

[3] A.B. Henriques and L.C.D. Gonçalves, Semicond. Sci. Technol. **8**, 585 (1993).

[4] A.B. Henriques and L.C.D. Gonçalves (unpublished); Surf. Sci. (to be published).

[5] Tan Le, A.G. Norman, W.T. Yuen, L. Hart, I.T. Ferguson, J.J. Harris, C.C. Philips, and R.A. Stradling (unpublished).

[6] M.H. Cohen and L.M. Falicov, Phys. Rev. Lett. **7**, 231 (1961).

[7]A.B. Henriques (unpublished).
[8]S. Yamada and T. Makimoto, Appl. Phys. Lett. **57**, 1022 (1990).
[9]A.B. Pippard, Proc. R. Soc. London, Ser. A **270**, 1 (1962).
[10]R.W. Stark and L.M. Falicov, Prog. Low Temp. Phys. **5**, 235 (1967).
[11]R.C. Young, J. Phys. C **4**, 458 (1971).
[12]M.I. Kaganov and A.A. Slutskin, Phys. Rep. **98**, 190 (1983); A.A. Slutskin and L.Yu. Gorelik, Solid State Commun. **46**, 601 (1983).
[13]V.A. Bondar, V.N. Morgoon, and V.I. Nizhankovskii, Zh. Eksp. Teor. Fiz. **94**, 130 (1988) [Sov. Phys. JETP **67**, 9158 (1988)].